JOURNAL OF PHYSICAL ORGANIC CHEMISTRY, VOL. 10, 577–584 (1997)

KINETIC, THERMODYNAMIC AND MECHANISTIC STUDIES ON THE REDUCTION OF CARBENIUM IONS BY NAD(P)H ANALOGUES

JIN-PEI CHENG* AND YUN LU
Department of Chemistry, Nankai University, Tianjin 300071, China

Hydride transfer mechanisms of the reductions of xanthylium ion by NAD(P)H analogues (i.e. BNAH, HEH and $AcrH_2$) were investigated. Both the kinetic observations and an analysis of thermodynamic driving forces for each mechanistic step in all the possible mechanisms indicate that the reductions are initiated by a rate-determining electron transfer, followed by a fast hydrogen atom abstraction. The mechanism of the reductions of 9-phenylxanthylium and triphenylmethylium ions by BNAH were also investigated and are similarly discussed. © 1997 John Wiley & Sons, Ltd.

J. Phys. Org. Chem. **10**, 577–584 (1997) No. of Figures: 4 No. of Tables: 4 No. of References: 26
Keywords: carbenium ions; reduction; NAD(P)H analogues
Received 23 September 1996; revised 30 January 1997; accepted 6 February 1997

INTRODUCTION

The mechanisms of NAD(P)H model-mediated reductions have long been a subject of extensive investigations owing to their potential linkage to the *in vivo* situation for many biological functions of this coenzyme. Two different types of mechanisms have been proposed to describe this reduction, i.e. the one-step hydride transfer and the multi-step hydride transfer, which is initiated first by an electron transfer (i.e. $e^- - H^+ - e^-$ or $e^- - H^\bullet$ pathways).[1] As early as 1955, Mauzerall and Westheimer[2] provided evidence to show that the hydride ion was directly transferred from a simple model, 1-benzyl-1,4-dihydronicotinamide (BNAH), to the substrates in reductions of malachite green and thiobenzophenones. Later, however, the generality of this one-step mechanism was questioned by others since the hydrogen exchange at the C-4 atom of the model molecule with hydrogens in solvent was observed in the reductions of arenediazonium[3] and thiobenzophenones.[4] In addition, it is also reported that primary kinetic isotope effect was found to be much smaller than the isotope ratio found in product in the reduction of α,α,α-triflurophenone with 1-propyl-1,4-dihydronicotinamide, suggesting that the reaction may proceed via a charge-transfer complex transition state (T.S.) rather than a simple hydride transfer T.S.[5] These observations, together with other evidence collected by means of kinetic,[6a–c] thermodynamic[6d] and product analysis[6e] as well as by ESR,[6f] UV[6g] and CIDNP[6h] techniques, suggest that the apparent hydride transfer may be a result of a transfer sequence including electron–proton–electron transfer or electron–hydrogen atom transfer.

Although most of the existing evidence seems to be in favor of the multi-step pathways, controversies about the two types of mechanisms have not been solved. For example, Yausi and Ohno[7] indicated that distinct electron transfer occurs only under electro- or photochemical conditions. Powell and Bruice[8] and Carlson *et al*.[9] pointed out that the exclusive electron transfer is significant only when the substrate can be readily reduced (i.e. possesses a high reduction potential). In an effort to combine these two mechanisms, Bunting[10] recently suggested that the two kinds of transfers be merged into a unified mechanism in terms of an imbalanced development of electronic charge and C–H bond fission in the transition state. All these arguments reveal that there is still considerable debate on the mechanistic details of reductions mediated by NAD(P)H models.

Kinetic or thermodynamic parameters, especially a combination of the two, are believed to be most useful in evaluating mechanisms for many types of organic reactions. However, to our knowledge, no thermodynamic details in a single solvent about the reductions mediated by NAD(P)H models have been reported, mostly due to the transient nature of the intermediate species involved in each step of the reduction. In this paper, we report the first estimates of the thermodynamic driving forces (Gibbs free energy) for each individual steps as shown in Scheme 1 for the reductions of xanthylium ions (Xn^+ and 9-$PhXn^+$) and trityl cation by NAD(P)H models including BNAH and 10-methyl-9,10-dihydroacridine ($AcrH_2$). The second-order rate constants, kinetic isotope effects, activation parameters and radical inhibitor effect for the reductions by BNAH,

* *Correspondence to:* J.-P. Cheng.
Contract grant sponsor: Natural Science Foundation of China.

 CCC 0894–3230/97/070577–08 $17.50

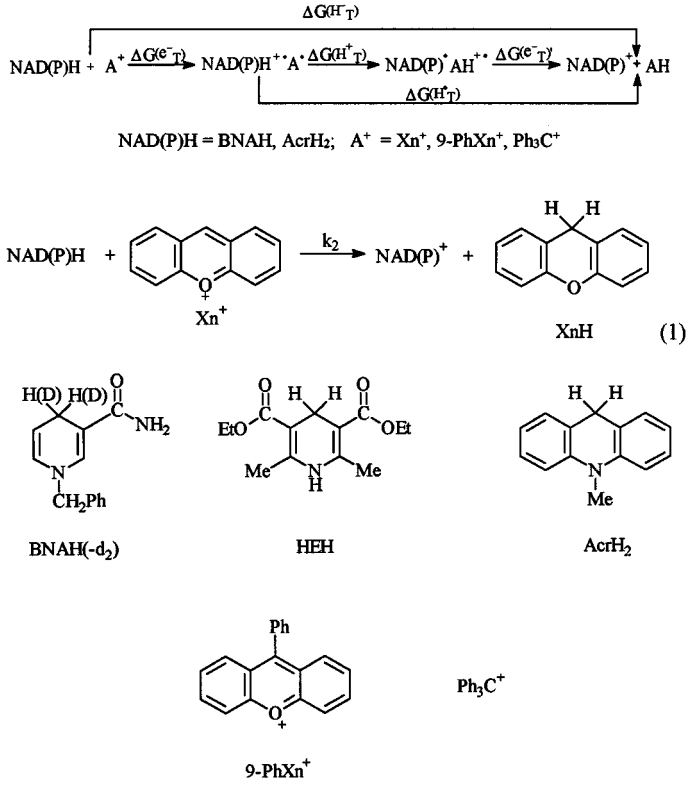

Scheme 1

$AcrH_2$ and Hantzsch ester (HEH) have also been investigated [equation (1)]. Free energy changes (ΔG) of each of the primary steps in various mechanisms (Scheme 1) were derived through appropriate thermochemical cycles (see Results section) by combining pK_a values and the relevant redox data for the species involved. Based on these measurements, a reasonable mechanism is suggested for the reduction of Xn^+ by the NAD(P)H models used in this work. The mechanism for the reductions of 9-phenylxanthylium (9-$PhXn^+$) and triphenylmethylium (Ph_3C^+) ions with BNAH is also presented according to a similar analytical strategy.

EXPERIMENTAL

Materials. 1-Benzylnicotinamide bromide (BNA^+), 1-benzyl-1,4-dihydronicotinamide (BNAH) and its 4,4′-dideuterated analogue (BNAH-d_2) were prepared according to the procedure in literature.[11] *N*-Methylacridinium ion ($AcrH^+$) and 10-methyl-9,10-dihydroacridine ($AcrH_2$) were obtained by the method as described in Ref. 12. Hantzsch ester (HEH) was synthesized by a general procedure.[13] Xanthydrol was obtained from Aldrich and recrystallized from aqueous ethanol. 9-Phenylxanthylium and trityl ions were prepared by dehydroxylation of 9-phenylxanthenol (Aldrich) and triphenylmethanol (Aldrich), respectively, with 48% HBF_4 in $(CH_3CH_2CO_2)_2O$.[14] All the compounds synthesized in this work were characterized by verifying their melting points using a Yanaco micro melting-point apparatus (uncorrected) and by the ^1H NMR spectra recorded on a JEOL 90Q NMR spectrometer. Acetonitrile (spectroscopic grade) was refluxed over $KMnO_4$ and K_2CO_3 for several hours and was doubly redistilled before use. The 30% CH_3CN–70% H_2O phosphate buffer was adjusted to pH 6·90 at different temperatures on a Beckman ϕ 71 pH meter which was calibrated by a general method prior to use. The *o*-phthalate buffer was similarly treated and was adjusted to pH 4·00. Purification of DMSO solvent and preparation of dimsyl base ($CH_3SOCH_2^-K^+$) were carried out according to the standard procedure.[15] Commercial tetrabutylammonium hexafluorophosphate (Bu_4NPF_6, Aldrich) was recrystallized from CH_2Cl_2 and vacuum dried at 110 °C overnight before preparation of the supporting electrolyte solution.

Reduction of 9-phenylxanthylium and trityl cations by BNAH. To a mixture of carbenium ion (0·5 mmol) and BNAH (0·5 mmol) was added 3 ml of deaerated acetonitrile containing 0·5 ml of CF_3COOD in the dark under argon. Ten minutes later, water was added to quench the reaction. The

product mixture was extracted with benzene and was isolated by preparative TLC to give 9-phenylxanthene (9-pHXnH) (62%) as the sole product, m.p. 142·0–143·0 °C (CRC, 145·0–146·0 °C); ^{1}H NMR (δ $CDCl_3$), 7·01–7·52 (m, 13H), 5·32–5·41 (s, 1H). For the latter case, triphenylmethane (Ph_3CH) (50%) was isolated, m.p. 91·0–93·0 °C (Aldrich, 93–94 °C); ^{1}H NMR (δ, $CDCl_3$), 7·09–7·53 (m, 15H), 5·58–5·65 (s, 1H).

Kinetics. The kinetic data were obtained in 30% CH_3CN–70% H_2O (v/v) at pH 6·90 (phosphate buffer) and an ionic strength of 1·0 (KCl) for the reductions of Xn^+ with BNAH and HEH or at pH 4·00 (*o*-phthalate buffer) with $AcrH_2$ at a certain temperature. The reactions were followed by monitoring the changes in absorbance at 358 nm for BNAH, 365 nm for HEH and 450 nm for *N*-methylacridinium ion ($AcrH^+$) under pseudo-first-order conditions (20–100-fold excesses of xanthydrol). The concentrations of BNAH, HEH and $AcrH_2$ were 0·04, 0·04 and 0·02 mM, respectively. In a typical run, xanthydrol (XnOH) solution of a certain concentration was first placed in a thermostatic bath for 15 min at 25 °C. Then 2·5 ml of solution were delivered into a UV cell (10 mm path). The cell was sealed with a silicon-rubber stopper and placed in a cell compartment maintained at 25 °C for another 15 min. Then 10 μl of 0·01 M BNAH solution in acetonitrile were injected into the cell.

Immediately after thorough mixing of the reactants, the changes in absorption at 358 nm vs time were recorded on a Beckman DU-8B UV–VIS spectrophotometer. Pseudo-first-order rate constants (k_{obs}) were calculated according to Guggenheim's method as described in the equations

$$-\ln(A_t - A_{t+\Delta}) = k_{obs}t + C \quad (2)$$

$$-\ln(A_{t+\Delta} - A_t) = k_{obs}t + C \quad (3)$$

where A_t and $A_{t+\Delta}$ represent absorbances at time t and $t+\Delta$ (Δ was generally 1—3 half-times), respectively. The data were treated by linesar regression and the correlation coefficients were always better than 0·999. The observed rate constant (k_{obs}) is the average of at least two independent runs. In the case where the reaction rate was taken in the presence of *m*-dinitrobenzene (DNB), a radical inhibitor, 15 μL of DNB in acetonitrile solution (0·5 M), was injected before BNAH was added.

Electrochemical measurements.[16] A 5 ml volume of a 2 mM solution of a substrate (i.e. BNAH, $AcrH_2$, BNA^+ or $AcrH^+$) in 0·1 M Bu_4NPF_6–DMSO was placed in an electrochemical cell under argon. The solution was bubbled with a small stream of argon both before and throughout the whole process. The cyclic voltagram (CV) was recorded at a sweep rate of 0·1 V s^{-1} on a BAS-100B electrochemical analyzer (Bioanalytical Systems, West Lafayette, IN, USA) equipped with a three-electrode assembly. The working electrode was a platinum disk (diameter 1 mm) and the reference electrode was 0·1 M $AgNO_3$/Ag prepared in 0·1 M Bu_4NPF_6–DMSO solution. The counter electrode was a platinum wire. The $AcrH^-$ anion was generated in DMSO by adding dimsyl base to a solution containing $AcrH_2$ (enough to produce 1 mM anion) under very strict air-tight conditions. Immediately after preparation of the anion, a CV was recorded by a similar procedure as described above. The ferrocenium/ferrocene (Fc^+/Fc) redox couple was taken as an internal standard in all cases.

RESULTS

Kinetics[17]

In aqueous solution, xanthylium cation is in equilibrium with its hydroxide adduct (xanthydrol, XnOH):

$$\begin{array}{l} Xn^+ + H_2O \overset{K_{R^+}}{\rightleftharpoons} XnOH + H^+ \\ \downarrow \quad k_2[BNAH] \\ XnH \end{array} \quad (4)$$

Therefore, the pseudo-first-order rate constant (k_{obs}) for reduction of xanthylium cation (Xn^+) by an NAD(P)H model can be evaluated by varying the concentration of XnOH at a certain temperature. In all cases, k_{obs} is found to be proportional to the substrate concentration ([XnOH]) (r>0·997). The apparent second-order rate constant (k_2^{app}) is then obtained from the slope of k_{obs} vs [XnOH]. The linear plots of k_{obs} vs [XnOH] for reductions of Xn^+ with BNAH and HEH at different temperatures are shown in Figure 1.

The pH-dependent pseudo-second-order rate constant (k_2) is defined by

$$-\frac{d[BNAH]}{dt} = k_2[Xn^+][BNAH]$$

$$= k_2 \frac{[H^+][XnOH]}{K_{R^+}[H_2O]}[BNAH]$$

$$= k_2^{app}[XnOH][BNAH] \quad (5)$$

$$k_2^{app} = k_2 \frac{[H^+]}{K_{R^+}[H_2O]} \quad (6)$$

$$\log k_2 = \log k_2^{app} - pK_{R^+} + pH \quad (7)$$

Since pK_{R^+} in 30% CH_3CN–70% H_2O is unknown, the exact second-order rate constant k_2 cannot be directly calculated, and therefore the k_2/K_{R^+} ratios for reduction of Xn^+ by BNAH and by its 4,4′-dideuterated analogue (BNAH-d_2) together with the apparent rate constant k_2^{app} are presented in Table 1. The relative rate measured in the presence of a radical inhibitor (*m*-dinitrobenzene, DNB) is also given.

The apparent rate constants (k_2^{app}) and the relative rate constants (k_2/K_{R^+}) of reductions of xanthylium ion by BNAH, HEH and $AcrH_2$ measured at different temperatures and the activation parameters calculated from the Erying slope and intercept [equation (8)] (r>0·995) jointly with

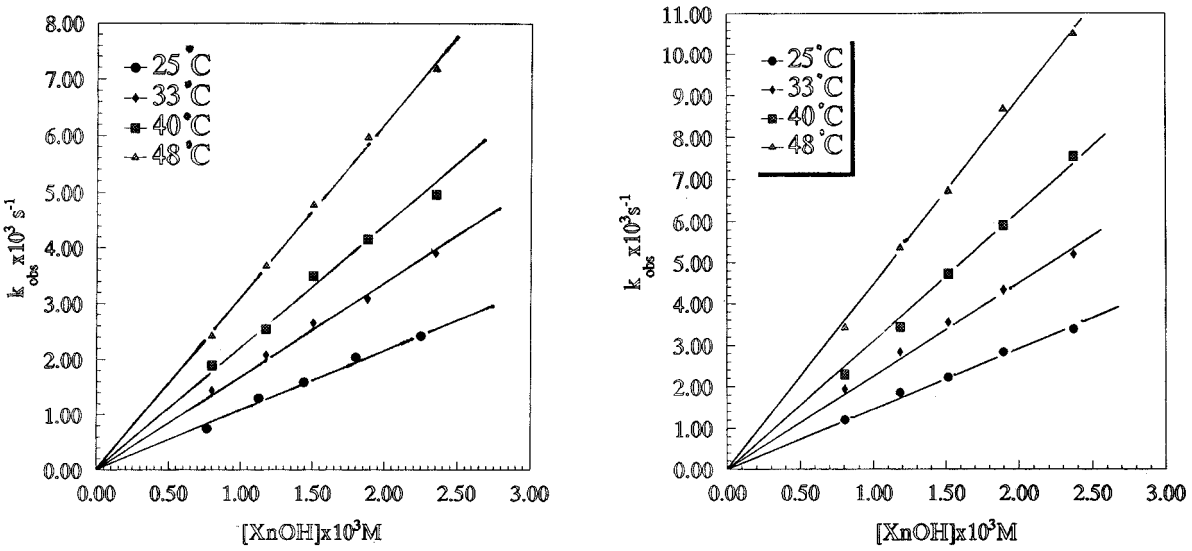

Figure 1. Linear correlations of k_{obs} vs [XnOH] in the reductions of Xn^+ by BNAH (0·04 mM) (left) and HEH (0·04 mM) (right) at 25, 33, 40 and 48 °C

equation (7) are summarized in Table 2.

$$\ln\left(\frac{k_2}{T}\right) = -\frac{\Delta H^{\neq}}{R}\frac{1}{T} + \frac{\Delta S^{\neq}}{R} + \ln\left(\frac{k_B}{h}\right) \quad (8)$$

Table 1. Relative second-order rate constants for the reduction of Xn^+ by BNAH[a]

Model	k_2^{app} ($M^{-1}\,s^{-1}$)	k_2/K_{R^+} ($M^{-1}\,s^{-1}$)	k_2^H/k_2^D
BNAH	1·12	$8·9\times10^6$	
BNAH-d_2	0·795	$6·3\times10^6$	1·4
BNAH+DNB	1·19	$9·4_5\times10^6$	

[a] In 30% CH_3CN–70% H_2O, pH = 6·90 and an ionic strength of 1·0 at 25 °C.

Thermodynamics

All the thermodynamic data were obtained at 25 °C in DMSO. Free energy changes for each individual primary steps for the e^-–H^+–e^- mechanism in Scheme 1 were estimated using the equations

$$\Delta G(e_T^-) = -F\Delta E[(A^+/A^{\bullet}) - (NAD(P)H^{+\bullet}/NAD(P)H)] \quad (9)$$

$$\Delta G(H_T^+) = 2·303RT[pK(NAD(P)H^{+\bullet}) - pK(AH^{+\bullet})] \quad (10)$$

$$\Delta G(e_T^-)' = -F\Delta E[(AH^{+\bullet}/AH) - (NAD(P)^+/NAD(P)^{\bullet})] \quad (11)$$

where $E(BNAH^{+\bullet}/BNAH)$, $E(AcrH_2^{+\bullet}/AcrH_2)$ and $E(XnH^{+\bullet}/XnH)$ are the oxidation potentials of BNAH, $AcrH_2$ and XnH, respectively and $E(BNA^+/BNA^{\bullet})$,

Table 2. Apparent second-order rate constants ($M^{-1}\,s^{-1}$) and relative rate constants ($M^{-1}\,s^{-1}$) at different temperatures and activation parameters of the reductions of Xn^+ by NAD(P)H models

	BNAH[a]		HEH[a]		$AcrH_2$[b]	
Temperature (K)	k_2^{app}	k_2/K_{R^+}	k_2^{app}	k_2/K_{R^+}	k_2^{app}	k_2/K_{R^+}
298·15	1·12	$8·9\times10^6$	1·39	$1·1\times10^7$	0·507	$5·1\times10^3$
306·15	1·58	$1·3\times10^7$	2·08	$1·7\times10^7$	0·878	$8·8\times10^3$
313·15	2·02	$1·6\times10^7$	3·37	$2·7\times10^7$	1·32	$1·3\times10^4$
321·15	3·09	$2·5\times10^7$	4·54	$3·6\times10^7$	2·39	$2·4\times10^4$
$\Delta H^{\neq}$ (kcal mol^{-1})	7·6		9·4		12·0	
$\Delta S^{\neq}$ (cal $mol^{-1}\,K^{-1}$)	$-1·3-4·6pK_{R^+}$		$5·2-4·6pK_{R^+}$		$-1·3-4·6pK_{R^+}$	

[a] In 30% CH_3CN–70% H_2O at pH = 6·90 and an ionic strength of 1·0.
[b] In 30% CH_3CN–70% H_2O at pH = 4·00 and an ionic strength of 1·0.

$E(\mathrm{AcrH^+/AcrH^\bullet})$ and $E(\mathrm{Xn^+/Xn^\bullet})$ are the reduction potentials of $\mathrm{BNA^+}$, $\mathrm{AcrH^+}$, and $\mathrm{Xn^+}$, respectively. The acid dissociation constants of radical cations, i.e. $pK(\mathrm{XnH^{+\bullet}})$ and $pK(\mathrm{AcrH_2^{+\bullet}})$, were obtained from a combination of $pK(\mathrm{AH})$ and oxidation potentials of the neutral molecule $[E_{ox}(\mathrm{AH})]$ and its conjugated base $[E_{ox}(\mathrm{A^-})]$ using the equation

$$pK(\mathrm{AH^{+\bullet}}) = pK(\mathrm{AH}) + F[E_{ox}(\mathrm{A^-}) - E_{ox}(\mathrm{AH})]/2{\cdot}303RT \quad (12)$$

where AH represents substrate $\mathrm{AcrH_2}$ or XnH.[16, 18–20] The acidity of radical cation derived from BNAH, i.e. $pK(\mathrm{BNAH^{+\bullet}})$, was estimated from the equation

$$pK(\mathrm{BNAH^{+\bullet}}) = [\Delta G_{BDE}\text{-}FE(\mathrm{BNAH^{+\bullet}/BNAH}) + FE(\mathrm{H^+/H^\bullet})]/2.303RT \quad (13)$$

using a thermodynamic cycle as shown in Scheme 2. In equation (13), ΔG_{BDE} is the free energy change of C–H bond fission at the 4-position of BNAH and $E(\mathrm{H^+/H^\bullet})$ and $E(\mathrm{BNAH^{+\bullet}/BNAH})$ are the oxidation potentials of $\mathrm{H^\bullet}$ and BNAH, respectively.

Free energy changes of hydrogen atom transfer for the $\mathrm{e^-}$–$\mathrm{H^\bullet}$ mechanism and the direct one-step mechanism can be evaluated from equations (14) and (15), respectively, based on the thermodynamic cycles shown in Scheme 1.

$\mathrm{BNAH \rightarrow BNA^\bullet + H^\bullet}$	ΔG_{BDE}
$\mathrm{H^\bullet \rightarrow H^+ + e^-}$	$FE(\mathrm{H^+/H^\bullet})$
$\mathrm{BNAH^{+\bullet} + e^- \rightarrow BNAH}$	$-FE(\mathrm{BNAH^{+\bullet}/BNAH})$
$\mathrm{BNAH^{+\bullet} \rightarrow BNA^\bullet + H^+}$	$2{\cdot}303RTpK(\mathrm{BNAH^{+\bullet}})$

Scheme 2

$$\Delta G(\mathrm{H_T^\bullet}) = \Delta G(\mathrm{H_T^+}) + \Delta G(\mathrm{e_T^-})' \quad (14)$$

$$\Delta G(\mathrm{H_T^-})\Delta G(\mathrm{e_T^-}) + \Delta G(\mathrm{H_T^+}) + \Delta G(\mathrm{e_T^-})' \quad (15)$$

The basic data necessary for calculating the thermodynamic quantities of each primary mechanistic step and the free energy terms thus derived are listed in Tables 3 and 4, respectively.

DISCUSSION

Mechanism of the reduction of Xn^+ by BNAH

Examination of the data in Table 1 shows that there is essentially no primary kinetic isotope effect ($k_2^H/k_2^D = 1{\cdot}4$) in the reduction of Xn^+ by BNAH. This implies that electron transfer from BNAH to Xn^+ must be the rate-determining step. The small activation enthalpy of reduction ($\Delta H^{\neq} = 7{\cdot}6$ kcal mol^{-1} in Table 2) also indicates that the C–H bond fission at the 4-position of BNAH should not be much involved in the transition state. This mechanistic analysis can be further examined by comparing the free energy changes (driving forces) of each individual step for every possible mechanism (Scheme 1) of this reduction. From Table 4, it is conceivable that there are two feasible candidates (i.e. the $\mathrm{e^-}$–$\mathrm{H^\bullet}$ and $\mathrm{H^-}$ pathways) among the three reaction mechanisms listed for the reaction to proceed if based solely on the thermodynamic driving forces. The two consecutive endothermic reactions (i.e. $\mathrm{e_T^-}$ and $\mathrm{H_T^+}$) in the $\mathrm{e^-}$–$\mathrm{H^+}$–$\mathrm{e^-}$ multi-step hydride transfer mechanism make this route the least possible one for the reaction to choose. Further, since both the kinetic isotope experiment and the activation enthalpy value obtained in this work

Table 3. Acid dissociation constants of neutral substrates [pK(AH)] and the corresponding radical cations [$pK(\mathrm{AH^{+\bullet}})$] and redox potentials of the relevant species in DMSO at 25 °C

Compound (AH)	pK(AH)	$E_{ox}(\mathrm{A^-})$[a]	E_{ox}(AH)[a]	$E_{rd}(\mathrm{A^+})$[a]	$pK(\mathrm{AH^{+\bullet}})$
BNAH[b]			0·182	−1·528	−8[c]
$\mathrm{AcrH_2}$[b]	31·5[d]	−1·961[e]	0·497	−0·876	−10[f]
XnH[g]	30·0	−1·685	1·135	−0·293	−18
9-PhXnH[g]	27·9	−1·531	1·215	−0·366	−18
$\mathrm{Ph_3CH}$[g]	30·6	−1·486	1·415	−0·257	−18

[a] E^p values in volts referenced to the ferrocenium/ferrocene ($\mathrm{Fc^+/Fc}$) couple.
[b] This work.
[c] Calculated from equation (13), where ΔG_{BDE}, $E(\mathrm{BNAH^{+\bullet}/BNAH})$ and $E(\mathrm{H^+/H^\bullet})$ were taken as 263 kJ mol^{-1} (estimated from known values of structurally similar molecules;[16, 18–20] the error is probably within ±10 kJ mol^{-1}), 0·72 V (value from Table 3 adjusted to vs NHE by adding 0·537 V) and −2·48 V (vs NHE),[21] respectively.
[d] Estimated value based on the pK_as of similar structures.
[e] Appeared as a shoulder.
[f] Calculated from equation (12).
[g] From Refs 19 and 22; values were adjusted to vs $\mathrm{Fc^+/Fc}$ (from a value vs NHE by subtracting 0·537 V when necessary).

Table 4. Free energy changes (kcal mol^{-1}) of each mechanistic steps for various hydride transfer mechanisms shown in Scheme 1[a]

	Mechanism					
	e^-–H^+–e^-			e^-–$H^\bullet$		H^-
Model/substance	$\Delta G(e_T^-)$	$\Delta G(H_T^+)$	$\Delta G(e_T^-)'$	$\Delta G(e_T^-)$	$\Delta G(H_T^\bullet)$	$\Delta G(H_T^-)$
BNAH/Xn^+	11·0	13·7	−61·4	11·0	−47·7	−36·7
$AcrH_2$/Xn^+	18·2	11·0	−46·4	18·2	−35·4	−17·2
BNAH/9-PhXn^+	12·6	13·7	−63·3	12·6	−49·6	−37·0
BNAH/Ph_3C^+	10·1	13·7	−67·9	10·1	−54·2	−44·1

[a] All values are derived in DMSO at 25 °C using equations (9)–(11), (14) and (15).

appeared to disfavor the one-step hydride transfer (i.e. H_T^-) mechanism, the e^-–$H^\bullet$ two-step hydride transfer can thus be assigned as the mechanism for the reduction of Xn^+ cation by BNAH.

The observation that the rate of reduction remains virtually unchanged in the presence of a radical inhibitor (see entry 3 in Table 1) seems at first glance to conflict with the radical mechanism mentioned above. However, it is generally understood that if the radical formed is too unstable to escape from the solvent cage or, in other words, the follow-up reaction within the cage is too fast to allow the incipient radical to move out of the solvent cage, the absence of the ESR signal or radical inhibitor effect could not then be taken as a criterion to exclude the radical mechanism. In fact, the follow-up hydrogen atom transfer ($H_T^\bullet$) in the e^-–$H^\bullet$ mechanism is indeed evaluated as extremely exothermic [$\Delta G(H_T^\bullet) = -47{\cdot}7$ kcal mol^{-1}], and therefore it is conceivable that there should be no chance for the DNB molecule to trap either the $Xn^\bullet$ radical or the $BNAH^{+\bullet}$ radical cation before a hydrogen atom is transferred within the encounter complex. In other words, the multi-step mechanism does not necessarily mean that the hydrogen transfer in the e^-–$H^\bullet$ mechanism is completely separated from the initial electron transfer, i.e. the barrier for the electron transfer is possibly overlapped with the follow-up hydrogen transfer in the reaction coordinate. Hence the DNB molecule could not serve as a radical trapper in such circumstances.

As mentioned previously (Results section), since that the pK_{R^+} value in the present working solvent (30% CH_3CN–70% H_2O) is unknown, the second-order rate constant of the reduction can only be derived in a relative form as k_2/K_{R^+} (Table 1). However, if we assume that the pK_{R^+} here is the same as that in water ($-0{\cdot}83$[22a]), then $k_2 = 6{\cdot}0 \times 10^7$ M^{-1} s^{-1} can be immediately evaluated from equation (7) for reduction of Xn^+ by BNAH, which agrees well with that previously reported by Bunting and Conn[17] ($5{\cdot}9 \times 10^7$ M^{-1} s^{-1}). It should be pointed out that there is an unknown amount of uncertainty associated with this k_2 value due to the change of the solvent (we are grateful to a referee for bringing this to our attention), and therefore the k_2 of $6{\cdot}0 \times 10^7$ M^{-1} s^{-1} and also all other literature rate data similarly derived can only be considered as the rate maxima. This is because the proton, a product in the equilibrium depicted in equation (4), is better solvated by H_2O than by MeCN, and this will shift the equilibrium to the left in the case where a mixed solvent is used and thus lead to a substantial deduction of the apparent K_{R^+}. Hence the K_{R^+} value in neat water is at its maximum and so is k_2 in water. On the other hand, $\Delta S^{\neq}$ of this reaction should not exceed 2·3 e.u. (derived assuming $pK_{R^+} = -0{\cdot}83$) for the same reason.

Based on the considerations discussed above, the mechanism of the reduction of xanthylium ion by BNAH can be proposed as the following sequence, i.e. (i) a fast pre-equilibrium between BNAH and Xn^+, (ii) a rate-determining electron transfer within an encounter complex leading to $BNAH^{+\bullet}$ and $Xn^\bullet$ and (iii) a fast hydrogen atom transfer from $BNAH^{+\bullet}$ to $Xn^\bullet$ to form the final products BNA^+ and XnH. The mechanism is illustrated in Scheme 3.

Reduction of Xn^+ by HEH and $AcrH_2$

Similarly to the situation for the reduction of Xn^+ by BNAH, the largely exothermic hydrogen atom transfer [$\Delta G(H_T^\bullet) = -35{\cdot}4$ kcal mol^{-1} in Table 4] can also initiate an endothermic electron transfer to occur in the reduction of Xn^+ by $AcrH_2$. Hence the two-step e^-–$H^\bullet$ mechanism is also applied, although in this case the relative second-order rate constant ($k_2/K_{R^+} = 5{\cdot}1 \times 10^3$ M^{-1} s^{-1} at 25 °C) derived from equation (6) is over 1000 times smaller than that of BNAH ($k_2/K_{R^+} = 8{\cdot}9 \times 10^6$ M^{-1} s^{-1}), due primarily to the difference of their oxidation potentials ($E_{ox} = 0{\cdot}182$ and 0·497 V, respectively; Table 3). The difference in the electron-donating abilities of $AcrH_2$ and BNAH can also be reflected kinetically by the 4·4 kcal mol^{-1} difference in their activation enthalpies ($\Delta H^{\neq} = 12{\cdot}0$ vs 7·6 kcal mol^{-1} in Table 2), since the activation entropies of these two reactions are almost identical. On the other hand, it is interesting that the Hantzsch ester (HEH), a reductant of similar electron-donating ability to $AcrH_2$ ($E_{ox} = 0{\cdot}446$ V[23] and 0·497 V, respectively), actually reacts much faster than the latter (see Table 2). The reduction rates by HEH are even *faster* than

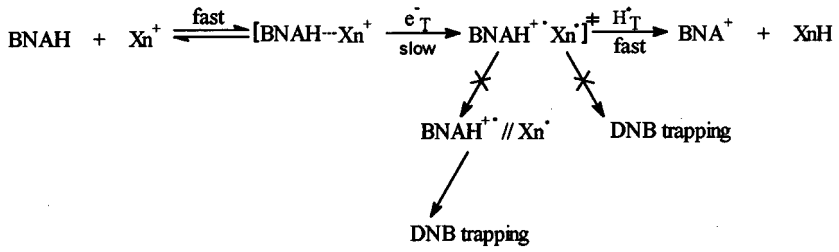

Scheme 3

those by BNAH for all the temperatures examined (Table 2). This may seem surprising if only the thermodynamic driving force (i.e. E_{ox}) is considered to affect the reaction, because HEH is actually a poorer electron donor than BNAH (E_{ox} = 0·446 and 0·182 V, respectively). From the activation parameters in Table 2, one can immediately see that the entropy of activation of HEH is 6·5 e.u. less negative ($\Delta S^{\neq} = 5{\cdot}2 - 4{\cdot}6\, pK_{R^+}$) than those of the other two models ($\Delta S^{\neq} = -1{\cdot}3 - 4{\cdot}6\, pK_{R^+}$). Hence the smaller entropy loss for the former reaction must be a cause of its higher rate. On the other hand, another point worth mentioning is that the difference in the activation enthalpies between HEH and BNAH ($\Delta\Delta H^{\neq} = 1{\cdot}8$ kcal mol^{-1}) is notably smaller than the difference in their oxidation potentials ($\Delta E_{ox} = 0{\cdot}264$ V = 6·1 kcal mol^{-1}). In other words, the energy gap between these two model compounds on going from the neutral molecule to its oxidized form (i.e. HEH$^{+\bullet}$ and BNAH$^{+\bullet}$) is attenuated in the T.S. compared with its initial state. The cause of the gap attenuation is most likely the enhanced electrostatic association of HEH with Xn$^+$ (presumably through the carbonyl group) within the encounter complex compared with that with BNAH, since HEH bears two linker groups (i.e. carbonyl) whereas BNAH has only one. This type of electrostatic interaction has already been proposed previously by others based on quantum mechanical calculations[24] and should contribute in part, together with the above-mentioned favorable entropy of activation for HEH, to the reversion of the order of their thermodynamic driving forces (BNAH > HEH) to the observed order of reactivity (HEH > BNAH). In the cases when no linker group exists (e.g. AcrH$_2$/Xn$^+$), the π–π interaction may contribute most to stabilization of the T.S., which is similar to the situation reported in the literature.[11] According to these analyses, the encounter complex formed prior to the rate-determining electron transfer must be productive rather than non-productive.[11]

From the above discussions, it now becomes clear that the thermodynamic driving force is not often the only factor influencing the kinetics and, as in the case of the present study, the entropy effect and the electrostatic interaction in the T.S. may play an important role in relating the thermodynamic quantities with kinetic behavior. We think that it is very likely for the NAD(P)H-type reductions that the above-mentioned two types of effects may in some sense be related to the well known term 'reorganization energy (λ)′ in the Marcus equation,[25] although the latter term certainly covers a much wider range of applications and deserves much more detailed theoretical considerations.

Reductions of 9-phenylxanthylium (9-PhXn$^+$) and trityl cations (Ph$_3$C$^+$) by BNAH

Examination of entries 3 and 4 in Table 4 reveals that the free energy changes of each individual steps in every possible mechanism for reductions of 9-PhXn$^+$ and Ph$_3$C$^+$ by BNAH have a similar pattern to those observed in the reduction of Xn$^+$ by BNAH. This implies that the apparent hydride transfer in these two reductions is again initiated by a rate-determining electron transfer followed by a fast hydrogen atom abstraction. The failure to obtain a deuterated product (i.e. 9-PhXnD or Ph$_3$CD) upon addition of deuterated trifluoroacetic acid (CF$_3$COOD) to the reaction system indicates that the hydrogen transfer may not be fully separated from the initial electron transfer, a situation similar to that described earlier for the reduction of Xn$^+$ by the same model compound. This also explains why the kinetics of the reduction of Ph$_3$C$^+$ with BNAH do not change in the presence of oxygen.[26]

CONCLUSION

Kinetic quantities such as rate constants, activation parameters and isotope effects for the NAD(P)H model-mediated reductions of some carbenium ions were investigated. The thermodynamic driving forces (i.e. Gibbs free energy changes) of every mechanistically possible primary step for the overall hydride transfer reactions were derived. The results suggest that all the apparent hydride transfer reactions studied here are possibly initiated by a rate-limiting electron transfer followed by a very fast hydrogen atom transfer. The molecular binding forces within the encounter complex of HEH/Xn$^+$, which presumably originated from the electrostatic association between the two reactants through a carbonyl linkage, together with its favorable activation entropy, may be responsible for reverting the order of the thermodynamic driving forces (BNAH > HEH) to the observed order of reactivity (HEH > BNAH).

ACKNOWLEDGMENT

This research was made possible by a grant from the Natural Science Foundation of China (NSFC), to whom the authors express their sincere gratitude.

REFERENCES

1. S. Fukuzumi, S. Koumitsu, K. Hironaka and T. Tanaka, *J. Am. Chem. Soc.* **109**, 305–316 (1987), and references cited therein.
2. D. Mauzerall and F. H. Westheimer, *J. Am. Chem. Soc.* **77**, 2261–2264 (1955).
3. S. Yasui, K. Nakamura and A. Ohno, *J. Org. Chem.* **49**, 878–882 (1984).
4. S. Yausi, K. Nakamura, A. Ohno and S. Oka, *Bull. Chem. Soc. Jpn.* **55**, 196–199 (1982).
5. J. J. Steffens and D. M. Chipman, *J. Am. Chem. Soc.* **93**, 6694–6696 (1971).
6. (a) M. F. Powell, J. C. Wu and T. C. Bruice, *J. Am. Chem. Soc.* **106**, 3850–3856 (1984); (b) B. W. Carlson and L. L. Miller, *J. Am. Chem. Soc.* **105**, 7453–7454 (1983); (c) S. Fukuzumi and Y. Tokuda, *J. Phys. Chem.* **97**, 3738–3741 (1993); (d) J.-M. Saveant, *Acc. Chem. Res.* **26**, 455–461 (1993); (e) W. Adam, M. Heil and R. Hutterer, *J. Org. Chem.* **57**, 4491–4495 (1992); (f) Y. Ohnishi and A. Ohno, *Chem. Lett.* 697–700 (1976); (g) A. Ohno, H. Yamamoto and S. Oka, *Bull. Chem. Soc. Jpn.* **54**, 3489–3491 (1981); (h) S. Fukuzumi and M. Chiba, *J. Chem. Soc., Perkin Trans. 2*, 1393–1398 (1991).
7. S. Yausi and A. Ohno, *Bioorg. chem.* **14**, 70–96 (1986).
8. M. F. Powell and T. C. Bruice, *J. Am. Chem. Soc.* **105**, 1014–1021, 7139–7149 (1983).
9. B. W. Carlson, L. L. Miller, P. Neta and J. Grodkowski, *J. Am. Chem. Soc.* **106**, 7233–7239 (1984).
10. J. W. Bunting, *Bioorg. Chem.* **19**, 456–491 (1991).
11. J. W. Bunting and S. Sindhuatmadji, *J. Org. Chem.* **46**, 4211–4219 (1981).
12. R. M. G. Roberts, D. Ostovic and M. M. Kreevoy, *J. Org. Chem.* **48**, 2053–2056 (1983).
13. A. Singer and M. McElvain, *Org. Synth.* **14**, 30–31 (1934).
14. H. J. Dauben, L. R. Honen and K. M. Harmon, *J. Org. Chem.* **25**, 1442–1445 (1960).
15. W. S. Matthews, J. E. Bares, J. E. Bartmess, F. G. Bordwell, F. G. Cornforth, G. E. Drucker, Z. Margolin, R. J. McCollum, G. J. McCollum and N. R. Vanier, *J. Am. Chem. Soc.* **97**, 7006–7014 (1975).
16. (a) J.-P. Cheng and Y. Zhao, *Tetrahedron* **121**, 5267–5276 (1994); (b) J.-P. Cheng, Y. Zhao and Z. Huan, *Sci. China (Ser. B)* **38**, 1417–1424 (1995).
17. J. W. Bunting and M. M. Conn, *Can. J. Chem.* **68**, 537–542 (1990).
18. A. M. P. Nicholas and D. R. Arnold, *Can. J. Chem.* **60**, 2165–2179 (1982).
19. J.-P. Cheng, PhD Dissertation, Northwestern University, Evanston, IL (1987).
20. (a) F. G. Bordwell and M. J. Bausch, *J. Am. Chem. Soc.* **108**, 2473–2474 (1986); (b) F. G. Bordwell, J.-P. Cheng and M. J. Bausch, *J. Am. Chem. Soc.* **110**, 2867–2872 (1988); (c) F. G. Bordwell, J.-P. Cheng and M. J. Bausch, *J. Am. Chem. Soc.* **110**, 2872–2877 (1988); (d) F. G. Bordwell and J.-P. Cheng, *J. Am. Chem. Soc.* **111**, 1792–1795 (1989).
21. V. D. Parker, *J. Am. Chem. Soc.* **114**, 7458–7462 (1992); **115**, 1201 (1993) (erratum).
22. (a) J.-P. Cheng, K. L. Handoo and V. D. Parker, *J. Am. Chem. Soc.* **115**, 2655–2660 (1993); (b) K. L. Handoo, J.-P. Cheng and V. D. Parker, *J. Am. Chem. Soc.* **115**, 5067–5072 (1993).
23. Unpublished results from this laboratory.
24. (a) M. C. A. Donkersloot and H. M. Buck, *J. Am. Chem. Soc.* **103**, 6554–6558 (1981); (b) Y.-D. Wu, D. K. W. Lai and K. N. Houk, *J. Am. Chem. Soc.* **117**, 4100–4108 (1995).
25. R. A. Marcus, *J. Phys. Chem.* **72**, 891–899 (1968).
26. M. Ishikawa, S. Fukuzumi, T. Goto and T. Tanaka, *Bull. Chem. Soc. Jpn.* **62**, 3754–3756 (1989).

